

An Efficient Implicit Scheme for the Simulation of Turbulent Combustion

M. Wasserman*

Corresponding author: markw@iscfdc.com

* Israeli CFD Center, Caesarea Industrial Park, Israel 3088900

Abstract: A robust numerical framework for the simulation of supersonic combustion is developed. The highly stiff reacting Reynolds-averaged-Navier-Stokes (RANS) equations are integrated in time using the extended unconditionally positive-convergent (UPC) implicit method. The iterative method is highly efficient thanks to a decoupled implicit solution of the mean-flow (Navier-Stokes) and chemical kinetics model equations, especially when large reaction mechanisms are employed. To complete the compact structure of the implicit UPC scheme, a diagonal approximation of the chemical reaction source-term Jacobian is proposed. The performance of the proposed implicit scheme is evaluated through simulation of supersonic, premixed and non-premixed combustion test cases. The obtained numerical results agree favorably with experimental measurements, and monotonic iterative convergence is demonstrated. Finally, the proposed diagonal scheme demonstrates considerable computational savings with respect to an equivalent scheme that is based on the full, analytic chemical reaction source-term Jacobian.

Keywords: Numerical Stiffness, Combustion, Implicit Schemes.

1 Introduction

Combusting flows are commonly found in modern engineering applications, such as high-speed propulsive systems (e.g., scram-jet engines) and atmospheric re-entry vehicles (RV). However, the accurate simulation and prediction of these flows presents a significant challenge to computational models, since it requires the modeling of finite rate chemical kinetics.

Chemically reacting flows may be generally classified based on the *Damköhler number*, representing the ratio of characteristic time scales of fluid motion and chemical reactions. When the Damköhler number is extremely large, chemical reactions progress at an infinitely fast rate, so the chemical composition of the gas adjusts immediately to changes in the flow, and the gas is assumed to be in *chemical equilibrium*. Alternatively, when the Damköhler number approaches zero, the time scale of the fastest chemical reaction is still considerably larger than that of the fluid motion. Therefore, the chemical composition does not respond to changes in the flow, and the gas is considered *chemically frozen*. The limiting cases of frozen and equilibrium flow are relatively easy to simulate with computational tools. However, most applications of interest require simulation of flows that are characterized by finite Damköhler numbers. These flows contain regions where chemical reactions do not reach equilibrium before the gas particles leave the reaction zone by means of convection. In such regions, the fluid is in a state of *chemical non-equilibrium* that may affect the surrounding flow by large density variations and heat release due to chemical reactions. The modeling of chemical non-equilibrium is considerably more complex, as it requires the calculation of instantaneous reaction rates from *chemical kinetics*.

1.1 Chemically Reacting Flow Modeling

The simulation of chemical non-equilibrium necessitates the use of finite-rate chemistry models to describe the kinetics of detailed reaction mechanisms. A single, global chemical reaction may qualitatively describe a complex process. Yet, accurate modeling of that process in a numerical simulation involves a break-down to numerous elementary reactions. Methane combustion, for example, takes place by a manifold of hundreds of elementary reactions, chemically equivalent to a single global reaction.

A chemical kinetics model allows to calculate the instantaneous kinetic rates of the elementary reactions comprising a specific detailed reaction mechanism. Several models usually exist for describing the same reaction mechanism, varying in accuracy and complexity, where the latter is generally determined by the number of species and elementary reactions included in the model. This seemingly positive assortment of models also gives rise to one of the main difficulties in modeling chemically reacting flows - numerical results being highly sensitive to the choice of chemistry model. In a recent study, Tchuen and Zeitoun¹ compared several models for describing chemical reactions taking place in high-speed air flows. They were able to recognize differences of up to 10^6 [m^3/s] in the forward reaction rates suggested by the models for dissociation of nitrogen, leading to discrepancies of up to 20% in the shock stand-off distance in a Mach 15 flow past a blunt body. These discrepancies accentuate the importance of testing and choosing appropriate chemical kinetics models for specific applications.

The need to improve the understanding of complex flow physics drive the development of large detailed chemical kinetics models. Current state-of-the-art chemical kinetics models for combustion of hydrocarbon fuels already include more than 500 (!) species [2], each requiring the solution of a separate transport equation. Due to the fact that computational time increases significantly with the number of modeled species, modern CFD simulations are limited to either simple fuels, such as hydrogen, methane, and ethylene, that are described with smaller detailed mechanisms (less than 100 species) or to complex fuels such as propane, heptane, and JP-8 that are described with reduced mechanisms [3].

1.2 Numerical Difficulties

Chemically reacting flow simulations involve integration of the continuity, momentum, total energy conservation, and chemical species mass transport equations, which are partial differential equations (PDE) consisting of convection, diffusion, and source terms. The numerical integration of the equations governing such flows may be quite difficult for several reasons.

1.2.1 Numerical Stiffness

First and foremost, the integration of the equations is characterized by high *numerical stiffness*. A given set of differential equations is considered numerically stiff when the physical processes described by it (e.g., convection, diffusion, and chemical reaction) develop on very different time scales, or equivalently, when the corresponding eigenvalues of the discretized algebraic equation set vary greatly [4]. Unless properly treated, numerical stiffness may significantly limit iterative convergence rates of standard numerical methods and also result in lack of robustness of numerical simulations [5].

The numerical stiffness of the equations governing chemically reacting flows may be attributed to several factors. First, extremely dense meshing is commonly employed near solid walls to accurately resolve the thermal and kinetic boundary layers. This clustering of cells near the surface results in formation of highly stretched cells. As a result, the characteristic time scales of convection and diffusion processes may differ considerably, and the resulting eigenvalues of the system may be spread over a wide range of values. This effect may be noted even in certain non-reacting, laminar simulations.

Moreover, finite-rate chemistry and thermal non-equilibrium introduce severe numerical stiffness owing to the nature of source terms appearing in both models. The source terms representing the production and dissipation of vibrational energy, and the transformation of species due to chemical reactions, are often strongly nonlinear and contain time scales that greatly differ from those of the convective and diffusive terms. In addition, chemical kinetics is characterized by widely disparate time scales related to formation and

depletion of different species. In high-speed combustion of hydrogen with air, for instance, the characteristic time scales of hydroxyl (OH) formation are extremely short ($\sim 10^{-8}$ s), while the characteristic time scales of water vapor (H_2O) formation are relatively long ($\sim 10^{-2}$ s) [6]. It is this time-scale disparity that leads to numerical stiffness. To ensure stability and accuracy, any numerical method aimed at solving the NS equations coupled with chemical species mass and vibrational energy conservation equations should be able to consistently represent all the different time scales present in the flow. The most simple, yet restrictive means of complying with this requirement is to limit the allowed time-step by the rate of the fastest chemical reaction.

Another source of numerical stiffness lies in the boundary conditions for quantities that are nearly singular near solid boundaries, or admit rapid changes due to wall catalysis. Standard numerical approximation of near-wall derivatives of these quantities yields a significant error unless the near-wall grid spacing is extremely fine. Such grid spacing imposes severe restrictions on the maximum allowed local time step due to anisotropy, further aggravating numerical stiffness.

1.2.2 Computational Complexity

The system of the discrete equations governing chemically reacting flow may be very large, since the equations are solved for each cell in the computational domain. Furthermore, the inherent coupling between the equations for various cells, and among themselves, limits the use of parallelization and vectorization capabilities of modern high-performance computers for these problems. The large number of modeled chemical species, N_s , common in modern kinetics models, adds a substantial load, since the computational costs involved with implicit schemes for reacting flows normally scale with $O(N_s^3)$. When combined, these features of chemically reacting flow simulations impose severe requirements on the available computational resources, especially when traditional implicit schemes are employed.

1.2.3 Positivity

Lastly, in the process of convergence, non-physical solutions, namely negative values of species mass fractions, which are positive by virtue of the underlying physics, may appear. Loss of positivity of model variables may occur even in cases where an analytical solution exists and is guaranteed to remain positive [7].

The common technique to avoid non-physical, negative values of chemical species mass fractions is to employ artificial limiting by either allowing only positive increments, or by locally neglecting corrections that result in loss of positivity [8, 9]. This indeed guarantees that the iterative solution does not induce loss of positivity, but in regions where limiting is invoked, convergence rates often deteriorate.

To alleviate some of the numerical difficulties associated with positivity in turbulence models, Mor-Yossef and Levy [10, 11] presented a loosely coupled implicit time-integration scheme that ensures unconditional positivity and convergence, thanks to a special design of the implicit operator to form an M-matrix [12]. This method was successfully extended for use with finite-rate chemical kinetics models in this work.

1.3 Implicit Integration Schemes

A common approach for tackling some of the difficulties outlined in the previous subsection involves the use of implicit time-integration schemes. Chemical reactions generally evolve over characteristic times that are much shorter than those of the kinetic flow field. As a result, explicit numerical time integration schemes, which allow time steps proportional to the smallest time scale present in the flow, are inefficient in computing reacting flows. Instead, implicit schemes, which alleviate the strict time step limitations imposed due to stability considerations, are extensively used for numerical time integration of the stiff equation set governing chemically-reacting flows, and the accompanying model equations.

The belief that stiffness is related to the non-linear source terms led to the development of point-implicit [13] methods, where only the source terms are linearized in time, while the convective and diffusive terms are solved explicitly. This results in a compact, block-diagonal implicit Jacobian, which essentially rescales the time scale of chemical production so that it is of the same order as those of convection and diffusion,

in pseudo-time. Consequently, larger time-steps may indeed be used in cases where stiffness is entirely dominated by the source terms [14–16]. Unfortunately, in realistic viscous flows, numerical stiffness also originates from highly stretched grids, and anisotropy due to thin boundary layers. Therefore, the efficient solution of most flows of interest requires the use of fully implicit schemes, where all the terms are treated implicitly.

Fully implicit methods are widely used in the context of chemically reacting flows. The lower-upper symmetric successive over-relaxation (LU-SSOR) implicit scheme [17, 18] is a compact scheme in the sense that it only requires the inversion of a scalar tri-diagonal implicit operator for the convection and diffusion terms. However, both the LU-SSOR and its successor, the Lower-Upper Symmetric Gauss-Seidel (LU-SGS) [19] methods tend to exhibit poor convergence on highly stretched grids [20]. The data-parallel-line-relaxation (DPLR) method [20] is a massively-parallel extension of the Jacobi line solver, where the inversion is conducted along lines normal to the wall. The off-diagonal terms are relaxed through a series of parallel sub-iterations, thus reducing the cost of inverting the implicit operator. This approach is robust for a wide range of flows; however, its application to supersonic combustion may be limited, as a clear gradient direction where the off-diagonal terms may be relaxed does not always exist in such problems [21].

In both fully implicit and point-implicit schemes, the derivation of source term Jacobians is necessary. For arbitrary reaction mechanisms, including three-body reactions with varying third-body efficiencies, this may result in a large and highly populated implicit operator of size $(N_s \times N_s)$, where N_s again denotes the number of modeled species. Since implicit schemes require the inversion of Jacobian matrices at each time step, the computational cost of implicit reacting flow simulations normally scales quadratically with the number of species.

To afford simulations involving complex reaction schemes with hundreds of species, simplifications to the full source Jacobian are constantly sought. Park and Yoon [22] reduced the cost of inverting the source Jacobian by taking advantage of elemental mass conservation (i.e., sum of all species densities must equal the density of the fluid). Eberhardt and Imlay [23] proposed a diagonal approximation to the full source term Jacobian by replacing each diagonal term with the L_2 norm of the row, and zeroing the other elements in the row. This formulation is strictly diagonally dominant and thus stabilizes the numerical solution, at the account of convergence rates. Edwards²⁴ employed an approximate factorization of the full source term Jacobian to reduce the cost of the inversion, and Kim et al. [25, 26] have found that employing the diagonal or lower-triangular portions of the full source term Jacobian yielded better convergence and stability compared to those obtained with the full Jacobian. However, their findings were highly dependent on the species ordering, and thus are difficult to extend to arbitrary large reaction mechanisms. Katta and Roquemore [3] suggested to adopt only the stabilizing (negative) diagonal terms of the source term Jacobian in the implicit operator. By enhancing the diagonal dominance of the implicit operator, and avoiding the need to invert an $(N_s \times N_s)$ block matrix at each point, they were able to devise a robust method for simulations involving large chemical kinetics models. But, obviously, the added diagonal dominance somewhat hampers convergence rates in some cases. Recently, Lian et al. [27] studied the integration of problems with dominant source terms and showed improved convergence in RANS simulations with two-equation turbulence models. A simple manipulation of the positive part of the production term enabled an appropriate implicit treatment that maintains stability.

Another popular approach to alleviate the stiffness arising from chemical kinetics source terms is operator splitting [28], where the full chemistry operator is decomposed into a product of simpler operators. Operator-splitting schemes are usually based on the Strang splitting technique [29], wherein the chemical reaction source terms are separated from those of convection and diffusion. Such separation enables the use of relatively large time steps for the advection-diffusion portion of the chemistry model equations, and a robust solution of advection-reaction ordinary differential equations (ODE) via stiff ODE solvers [30, 31]. However, this technique does have a few major drawbacks. First, an error term due to splitting appears in the discretized equations, dependent on the time-step that is chosen for the computation [32]. This error term is in addition to the temporal and spatial discretization errors. Furthermore, even in a steady state simulation, growing modes, such as production of radical species, may require a limited time step due to accuracy requirements instead of stability requirements, thus lowering the advantage of having a large allowable time

step from stability considerations [33].

Many industrial CFD codes [20, 34, 35] solve the equations governing chemically reacting flow, including the Navier-Stokes, chemical kinetics, and possibly turbulence model equations, in a coupled manner. Namely, the turbulence model equations, species mass-conservation, momentum, and total energy equations are all solved simultaneously, resulting in a large system of equations, typically solved by inverting a block tri-diagonal matrix of $(N_s+7) \times (N_s+7)$ -sized blocks (in the case of two-equation turbulence models). Obviously, this approach incurs heavy computational costs, especially if the modeled reaction mechanism is very large. Recently, Candler et al. [36] proposed a decoupled implicit method where the chemistry model equations are solved separately from the Navier-Stokes equations, and only the diagonal portion of the source-term Jacobian is used in the implicit operator, while the off-diagonal elements are relaxed as described with the DPLR method. This resulted in a significant decrease in computational costs, given that the decoupled method converged in roughly the same number of steps as the fully coupled approach. However, as explained above, the use of the DPLR relaxation process may limit convergence rates in some cases, and is not generally suitable for combustion applications.

1.4 Scope

In a previous work [37], the unconditionally positive-convergent (UPC) time integration implicit scheme for turbulence transport equations [10] was successfully extended for use with chemical kinetics models. The extended UPC scheme ensures unconditional positivity of species mass fractions throughout the simulation. Consequently, the numerical difficulties associated with loss of positivity are alleviated without requiring artificial stabilization measures.

This work examines the advantages of a decoupled implicit method where the species mass transport model equations are solved separately from the Navier-Stokes equations, with regard to the conventional, fully coupled method, which incurs heavy computational costs, especially if the modeled reaction mechanism is very large. To maximize the computational savings offered by a decoupled implicit method, simplifications to the large, highly populated analytic chemical kinetics source term Jacobian are investigated. Special focus is given to the simulation of non-premixed, supersonic combustion which is considered highly stiff.

2 Governing Equations

In a compact, conservation-law form, the two-dimensional Favre-Reynolds-averaged Navier-Stokes (RANS) equations for a compressible, thermally perfect and reactive mixture of gases may be expressed in Cartesian coordinates as follows [38]:

$$\frac{\partial \mathcal{Q}}{\partial t} + \frac{\partial(\mathcal{F}_c - \mathcal{F}_d)}{\partial x} + \frac{\partial(\mathcal{G}_c - \mathcal{G}_d)}{\partial y} + \Phi(\mathcal{J}_c - \mathcal{J}_d) = \mathcal{S} \quad (1)$$

where $\Phi = 0$ in the general case of planar flow, and $\Phi = 1$ in the special case of axisymmetric flow (in the axisymmetric case, y denotes the radial direction). The vector $\mathcal{Q} = \{\mathbf{Q}, \mathbf{q}\}$ is composed of the dependent variables vector of the mean-flow equations, \mathbf{Q} , and of the $k - \omega$ turbulence and chemistry model equations, \mathbf{q} (hereinafter cumulatively referred to as *model equations*). These vectors are given as:

$$\mathbf{Q} = \begin{bmatrix} \rho \\ \rho u \\ \rho v \\ E \end{bmatrix}, \quad \mathbf{q} = \begin{bmatrix} \rho k \\ \rho \omega \\ \rho Y_1 \\ \vdots \\ \rho Y_{N_s-1} \end{bmatrix} \quad (2)$$

The mixture density is denoted by ρ , the Cartesian velocity vector components are denoted by u and v , and E denotes the total mixture energy. The turbulent kinetic energy is denoted by k , and the second turbulent

quantity is denoted by ω , representing the specific turbulent dissipation rate. The variables $Y_{s=1,\dots,N_s-1}$ denote the individual chemical species mass fractions.

The convective flux vectors are denoted by $\mathcal{F}_c = \{\mathbf{F}_c, \mathbf{f}_c\}$ and $\mathcal{G}_c = \{\mathbf{G}_c, \mathbf{g}_c\}$, where \mathbf{F}_c and \mathbf{G}_c are the convective flux vectors appearing in the mean-flow equations, and \mathbf{f}_c and \mathbf{g}_c are the convective flux vectors appearing in the model equations. The diffusive flux vectors are denoted as $\mathcal{F}_d = \{\mathbf{F}_d, \mathbf{f}_d\}$ and $\mathcal{G}_d = \{\mathbf{G}_d, \mathbf{g}_d\}$, where \mathbf{F}_d and \mathbf{G}_d are the diffusive flux vectors appearing in the mean-flow equations, and \mathbf{f}_d and \mathbf{g}_d are the diffusive flux vectors appearing in the model equations. The heat-flux terms are calculated based on Fourier's law, and Fick's law is employed to approximate the diffusion velocities of individual species.

The axisymmetric source terms are denoted by $\mathcal{J}_c = \{\mathbf{J}_c, \mathbf{j}_c\}$ and $\mathcal{J}_d = \{\mathbf{J}_d, \mathbf{j}_d\}$ where \mathbf{J}_c and \mathbf{J}_d are the source term vectors appearing in the mean-flow equations, and \mathbf{j}_c and \mathbf{j}_d are the source term vectors appearing in the model equations.

The mean-flow equations are closed using the equation of state for a mixture of thermally perfect gases (Dalton's law of partial pressures), given by:

$$p = \rho R_0 T \sum_{s=1}^{N_s} \frac{Y_s}{W_s} \quad (3)$$

where W_s is the molecular weight of species s , and R_0 is the universal gas constant. The total energy is then given by:

$$E = \sum_{s=1}^{N_s} \rho Y_s h_s - p + \frac{1}{2} \rho (u^2 + v^2) + \rho k \quad (4)$$

The source-term vector \mathcal{S} is represented by:

$$\mathcal{S} = [0, 0, 0, 0, S_k, S_w, S_1, S_2, \dots, S_{N_s-1}]^T \quad (5)$$

where S_k and S_w are the source terms appearing in the turbulence model equations, while $S_{s=1\dots N_s-1}$ are the source terms appearing in the mass conservation equations of the individual species (chemistry model equations).

2.1 Thermodynamic and Transport Properties

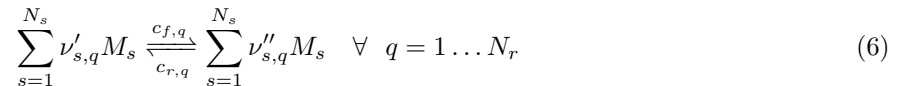
The viscosity coefficients of individual chemical species were approximated using Blottner's curve fits. The species thermal conductivity coefficients were calculated from their viscosity coefficients via the modified Eucken correction [39], with a Schmidt number of 0.7 as suggested by Reimann and Hannemann⁴⁰.

In all mechanisms examined in this work, Wilke's mixing rule was employed to calculate the mixture viscosity and conductivity [41]. Binary diffusion coefficients between species s and r , D_{sr} , are calculated according to the Chapman-Enskog theory, with Lennard-Jones potential and collision integrals from Refs. [42, 43]. An effective diffusion coefficient for individual species in a mixture is employed according to Ref. [44].

Nine-term polynomials of temperature are used for calculating the enthalpy, and the heat capacity at constant pressure of individual species [45]. Most of the above expressions include an explicit or implicit dependence on the temperature of the mixture, which is not readily available from the conservative variables, as in the non-reacting case. Instead, the temperature is calculated iteratively from the energy balance (see Eq. (4)) using a Newton-Raphson procedure.

2.2 Finite-rate Chemistry Model

A reaction mechanism composed of N_r reversible reactions may be generally described by the following chemical formulae:



where $\nu'_{s,q}$ and $\nu''_{s,q}$ are the stoichiometric coefficients of species s (represented by the chemical symbol M_s), acting as a reactant or product in reaction q , respectively. The current study was limited to flows in which the assumption of laminar chemistry holds. Accordingly, the Arrhenius approach may be used to describe the mean reaction rates (i.e., based only on mean values of temperature and species mass fractions). The formula for the mean reaction rate for species s , S_s , appearing in the above mechanism is then given by:

$$S_s = W_s \sum_{q=1}^{N_r} (\nu''_{s,q} - \nu'_{s,q}) \left[c_{f,q} \prod_{p=1}^{N_s} \left(\frac{\rho Y_p}{W_p} \right)^{\nu'_{p,q}} - c_{r,q} \prod_{p=1}^{N_s} \left(\frac{\rho Y_p}{W_p} \right)^{\nu''_{p,q}} \right] \quad (7)$$

where $c_{f,q}$ and $c_{r,q}$ are the forward and reverse rate coefficients of reaction q , respectively. These coefficients may be expressed in Arrhenius form as $c_q = A_q T^{\gamma_q} e^{-(E_q/R_0 T)}$, where γ_q and A_q are constants, and E_q is the activation energy.

Two different models for hydrogen combustion are considered; the first is a detailed, 9-species, 18-step model by Stahl and Warnatz [46], while the second is the 6-species, 8-reactions abridged Jachimowski model[47].

2.3 Turbulence Models

The averaging process for the Navier-Stokes equations described above results in some unknown quantities, for example, the Reynolds stress tensor. Modeling of these unknowns in terms of the averaged variables is required to close the system of equations. The unknown, Favre-averaged, Reynolds stress tensor is modeled in this work via the k - ω turbulence model developed by Kok⁴⁸, which is considered to be topology-free and was designed to resolve the well-known dependency on free-stream values of ω .

3 Numerical Method

This section describes the spatial and temporal discretizations employed in this work in order to enable the numerical solution of the continuous equations given in the previous section.

3.1 Finite-Volume Discretization

A conservative cell-centered finite volume methodology is employed to discretize the governing equations on structured grids. Let C_a denote a control area defined by a quadrilateral grid element, and let $\partial\Gamma$ denote the control area boundary, with $\mathbf{n} = [n_x, n_y]^T$ being the outward-pointing unit normal vector to $\partial\Gamma$. Integration of Eq. (1) over C_a , and application of the *Gauss theorem* results in the following integral form of the equations:

$$\frac{\partial}{\partial t} \int_{C_a} \mathcal{Q} \, dA + \int_{\partial\Gamma} (\mathcal{H}_c - \mathcal{H}_d) \, dl = \int_{C_a} (\mathcal{S} - \mathcal{S}_a) \, dA \quad (8)$$

where

$$\mathcal{H}_c = \mathcal{F}_c n_x + \mathcal{G}_c n_y \quad (9)$$

$$\mathcal{H}_d = \mathcal{F}_d n_x + \mathcal{G}_d n_y \quad (10)$$

are the fluxes normal to $\partial\Gamma$ and $\mathcal{S}_a = \Phi(\mathcal{J}_c - \mathcal{J}_d)$ is the axisymmetric source-terms vector. Let H_c and h_c denote the parts of \mathcal{H}_c associated with the mean-flow and model equations, respectively, and let H_d and h_d denote the analogous parts of \mathcal{H}_d , so that $\mathcal{H}_c = \{H_c^T, h_c^T\}^T$ and $\mathcal{H}_d = \{H_d^T, h_d^T\}^T$. Next, define

$$\mathcal{Q}_i = \frac{1}{A_i} \cdot \iint_{C_a} \mathcal{Q} \cdot dA$$

as the vector of cell-averaged conservative variables \mathcal{Q} inside cell i . Then, decomposition of the line integral to a sum of flux contributions on each of the four faces neighboring cell i results in the semi-discrete form of Eq. (8) for a non-deforming grid:

$$A_i \frac{d\mathcal{Q}_i}{dt} = - \sum_{j \in N(i)} (\mathcal{H}_{c_{ij}} - \mathcal{H}_{d_{ij}}) l_{ij} + (\mathcal{S}_i - \mathcal{S}_{a_i}) A_i \equiv \mathcal{R}_i \quad (11)$$

where the terms $\mathcal{H}_{c_{ij}}$ and $\mathcal{H}_{d_{ij}}$ are the discrete convective and diffusive fluxes, respectively, normal to the interface ij shared by cell i and one of its neighboring cell j , and \mathcal{S}_i , \mathcal{S}_{a_i} are the appropriate source-term vectors of cell i , and A_i is the cell area. The term l_{ij} is the face length of the interface ij , and $N(i)$ denotes the set of cell i 's neighbors (direct face neighbors). The vector,

$$\mathcal{R}_i = \{\mathbf{R}^T, \mathbf{r}^T\}_i^T$$

signifies the right hand side (residual) of the equation set, where \mathbf{R} represents the residual of the mean-flow equations, and \mathbf{r} represents the residual of the model equations. The discretization of the various terms (i.e., convective and diffusive fluxes and source-terms) appearing in the residual vector is discussed next.

The convective flux vector is computed at the cell interfaces using the AUSM-DV scheme [49]. A higher order of accuracy is achieved by applying a third-order, upwind-biased MUSCL interpolation method [50, 51], with the van-Albada limiter [52] as a means to suppress oscillations in the solution. The diffusive flux vector normal to the interface, \mathcal{H}_d , is calculated by employing second-order central differencing based on the diamond-shaped stencil [53].

3.2 Temporal Discretization

Implicit, pseudo-time marching of the discrete mean-flow, and model equations is employed, based on the first order backward Euler method:

$$A \frac{\Delta \mathcal{Q}}{\Delta \tau} = \mathcal{R}^{n+1} \approx \mathcal{R}^n + \left(\frac{\partial \mathcal{R}}{\partial \mathcal{Q}} \right)^n \Delta \mathcal{Q}^n, \quad n = 1, 2, \dots \quad (12)$$

where $\Delta = (\)^{n+1} - (\)^n$ is defined as the increment between time levels n and $n + 1$, $\frac{\partial \mathcal{R}}{\partial \mathcal{Q}}$ is the *Jacobian matrix* resulting from linearization of the residual, and $\Delta \tau$ is the local pseudo-time step, calculated from a CFL condition, as defined in Ref. [54]. Time-accurate simulations are achieved with dual-time marching.

Eq. (12) may be given in a compact, delta-form as follows:

$$\left[\frac{A}{\Delta \tau} \mathcal{I} - \frac{\partial \mathcal{R}}{\partial \mathcal{Q}} \right]^n \Delta \mathcal{Q}^n = \mathcal{R}^n \quad (13)$$

where \mathcal{I} is the identity matrix.

To improve iterative convergence to a steady-state solution, the B2 scheme proposed by Batten et al. [55] is employed. The B2 scheme is a modified variant of the backward Euler method. Denoting the pseudo-time integration process given in Eq. (13) by

$$\Delta \mathcal{Q}^n = B1(\mathcal{Q}^n, \Delta \tau) \implies \mathcal{Q}^{n+1} = \mathcal{Q}^n + \Delta \mathcal{Q}^n \quad (14)$$

the B2 scheme is defined as two successive modified B1 steps as follows:

$$\begin{aligned} 1st \ step: \quad \Delta \mathcal{Q}^* &= B1(\mathcal{Q}^n, \Delta \tau/2) \implies \mathcal{Q}^* = \mathcal{Q}^n + \Delta \mathcal{Q}^* \\ 2nd \ step: \quad \overline{\Delta \mathcal{Q}} &= B1(\mathcal{Q}^*, \Delta \tau) \implies \mathcal{Q}^{n+1} = \mathcal{Q}^* + \overline{\Delta \mathcal{Q}}/2 \end{aligned} \quad (15)$$

As pointed out by Batten et al. [55], the B2 scheme may alleviate convergence difficulties that are associated with the high-frequency fluctuations of limiters.

3.2.1 Loosely Coupled Time Integration

Eq. (13) is solved using the alternating line symmetric Gauss-Seidel method, in a loosely coupled manner. Loosely coupled time integration possesses several advantages over a coupled strategy. It is easy to implement and it provides the enhanced flexibility required to design a stable and efficient scheme for the model equations. In terms of stability, Wackers and Koren⁵⁶ showed that at the initial phase of a turbulent flow simulation, some of the eigenvalues of the linearized, fully coupled implicit operator have a negative real part, indicating an unstable scheme. In another study, Lee and Choi⁵⁷ conducted a linear stability analysis and concluded that there is no clear benefit to using a fully coupled time integration of the mean-flow equations and two-equation turbulence models over a loosely coupled approach. Moreover, for reacting flows, the loosely coupled approach offers a potential decrease in computational costs since its convergence properties were found similar to the fully coupled approach [36], while the cost per-iteration is significantly reduced thanks to sparsely-populated Jacobian matrices.

According to the loosely coupled approach, the implicit Jacobian is approximated as follows:

$$\left(\frac{\partial \mathcal{R}}{\partial \mathcal{Q}}\right)_{ij} = \begin{bmatrix} \left[\frac{\partial \mathbf{R}}{\partial \mathbf{Q}} \right]_{4 \times 4}, & \left[\frac{\partial \mathbf{R}}{\partial \mathbf{q}} \right]_{4 \times N_m}^{[0]} \\ \left[\frac{\partial \mathcal{R}}{\partial \mathbf{Q}} \right]_{N_m \times 4}^{[0]}, & \left[\frac{\partial \mathcal{R}}{\partial \mathbf{q}} \right]_{N_m \times N_m} \end{bmatrix}_{ij} \quad (16)$$

where $N_m = N_s - 1$ denotes the number of model equations solved.

It is important to note that coupling between mean-flow, and chemistry is only omitted in the process of deriving the Jacobian matrix, $\frac{\partial \mathcal{R}}{\partial \mathcal{Q}}$, that appears in the L.H.S (left-hand-side) of the equation set (13), while the R.H.S (right-hand-side) of the equations remains unchanged. In what follows, the separate, different implicit treatment of the mean-flow and the model equations is detailed.

3.2.2 Mean-Flow Equations Time Marching

The algebraic set of equations resulting from temporal and spatial discretization of the mean-flow equations may be written as:

$$\left[\frac{A}{\Delta \tau} \mathcal{I} - \frac{\partial \mathbf{R}}{\partial \mathbf{Q}} \right]^n \Delta \mathbf{Q}^n = \mathbf{R}^n \quad (17)$$

The evaluation of the exact Jacobian $\frac{\partial \mathbf{R}}{\partial \mathbf{Q}}$, of the high-order, nonlinear explicit operator \mathbf{R} is very complicated and may result in numerical instabilities [58]. To alleviate these difficulties, the common practice is to derive the Jacobian based on approximate expressions for the convective and diffusive flux terms. In this work, the contributions to the Jacobian of the mean-flow equations originating from the convective flux, hereinafter referred to as the “convective Jacobian”, are based on the first-order, Steger-Warming flux function [59]. The choice of a Steger-Warming-based Jacobian is motivated by the study of Amaladas and Kamath⁶⁰, who compared the performance of various Jacobians used in conjunction with the AUSM flux. A direct derivation of the split fluxes given in the Steger-Warming Flux-Vector-Splitting (FVS) scheme, with regard to Q_i and Q_j , respectively, is employed. This direct derivation approach was found to provide increased numerical stability [8] over that obtained when deriving the Jacobians based on the generally inaccurate extension of the homogeneous property of the analytic inviscid flux, H_c , to the split fluxes, H_c^\pm (i.e., $\frac{\partial H_c^\pm}{\partial Q} \approx A^\pm$).

To produce a compact stencil containing direct face neighbors only, the contributions to the Jacobian of the mean-flow equations originating from the diffusive flux, hereinafter referred to as the “diffusive Jacobian” are obtained by analytic derivation of the thin-layer-based, approximate flux. Moreover, the non-linear Reynolds-stress tensor that appears in the mean-flow equations is treated implicitly only with regard to its linear part.

3.2.3 Model Equations Time Marching

Similar to the mean-flow equations, the algebraic set of the discrete chemistry model equations is given by:

$$\left[\frac{A}{\Delta\tau} \mathcal{I} - \frac{\partial \mathbf{r}}{\partial \mathbf{q}} \right]^n \Delta \mathbf{q}^n = \mathbf{r}^n \quad (18)$$

The source terms appearing in the model equations are often strongly nonlinear and contain time scales that greatly differ from those of the convective and diffusive terms. As a result, the chemical kinetics model equations are generally highly stiff. Due to this stiffness, a straightforward implementation of the model equations' exact Jacobian, $\frac{\partial \mathbf{r}}{\partial \mathbf{q}}$, usually leads to an unstable scheme that exhibits convergence difficulties. Therefore, to increase the robustness of the numerical simulation, and to accelerate convergence, a highly-stable, implicit scheme for the model equations is sought.

The implicit scheme proposed by Mor-Yossef and Levy [10, 11] for two-equation turbulence models, which guarantees unconditional positivity of the transported variables and convergence of the fixed-point iteration on the linearized problem, was chosen in this work to tackle the numerical stiffness of the model equations. The scheme was successfully extended for use with finite-rate chemistry models in a previous work [37].

3.2.4 Implicit Treatment of Source-terms

For a complex reaction mechanism, the direct derivation of chemical kinetics source terms results in a large and generally dense implicit operator of size $(N_m) \times (N_m)$:

$$\frac{\partial \mathcal{S}}{\partial \mathbf{q}} = \begin{bmatrix} \frac{\partial S_1}{\partial (\rho Y_1)} & \cdots & \frac{\partial S_1}{\partial (\rho Y_{N_s-1})} \\ & \vdots & \\ \frac{\partial S_{N_s-1}}{\partial (\rho Y_1)} & \cdots & \frac{\partial S_{N_s-1}}{\partial (\rho Y_{N_s-1})} \end{bmatrix} \quad (19)$$

where $S_{i=1\dots N_s-1}$ denotes the chemical kinetics source term appearing in the mass conservation equation of species i . The inversion of such operators for each cell, and at each time step is often unaffordable in terms of computational complexity, especially when reaction schemes involving hundreds of species are employed. Therefore, simplifications to the full source-term Jacobian are sought. Keeping in mind that the UPC scheme provides diagonal implicit operators for the convective and diffusive fluxes, considerable savings in both memory and CPU time may be achieved if the implicit operator of the source-term, $\frac{\partial \mathcal{S}}{\partial \mathbf{q}}$, is constructed such that it is also diagonal. The following subsections are dedicated to the construction of the implicit operators.

3.2.5 Chemical Kinetics Source-terms

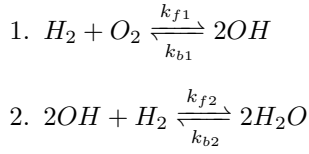
The analytic derivatives of the chemical kinetics source-terms, S_i , with respect to species j density are given by:

$$\begin{aligned} \frac{\partial S_i}{\partial (\rho Y_j)} = W_i \sum_{k=1}^{N_r} (\nu''_{i,k} - \nu'_{i,k}) & \left[\frac{\nu'_{j,k} c_{f,k}}{W_j} \left(\frac{\rho Y_j}{W_j} \right)^{\nu'_{j,k}-1} \prod_{l=1, l \neq j}^{N_s} \left(\frac{\rho Y_l}{W_l} \right)^{\nu'_{l,k}} - \right. \\ & \left. - \frac{\nu''_{j,l} c_{r,k}}{W_j} \left(\frac{\rho Y_j}{W_j} \right)^{\nu''_{j,k}-1} \prod_{l=1, l \neq j}^{N_s} \left(\frac{\rho Y_l}{W_l} \right)^{\nu''_{l,k}} \right] \end{aligned} \quad (20)$$

The resulting, full chemical kinetics source-term Jacobian is generally a dense matrix because any modeled species can theoretically react with all other species. Therefore, approximations of the full chemical source-term Jacobian have to be considered in order to sustain a diagonal implicit operator. Kim²⁵ and Kim et

al.²⁶ analyzed the eigenvalues of the full Jacobian in a constant volume reaction of hydrogen and oxygen, and found that they vary greatly and change sign throughout the simulation. Since the preferable time-integration method heavily depends on the sign of the eigenvalues of the Jacobian [27, 61], choosing an appropriate numerical procedure (i.e., explicit or implicit) for integration involving the full Jacobian may prove to be a difficult task. In contrast, when an approximate Jacobian is used, consisting of either the lower- or upper-triangular, or the diagonal portions of the full Jacobian, strictly negative eigenvalues appear throughout the simulation. As demonstrated below, this observation is true in most chemical reaction mechanisms thanks to the law of mass action resulting in a particular structure of the Jacobian.

For instance, examining a simplified, two-step model describing the combustion of hydrogen and oxygen [62]:



and applying the law of mass action to calculate the net rate of change of species densities, S , yields:

$$S_{O_2} = W_{O_2} (-k_{f1}C_{H_2}C_{O_2} + k_{b1}C_{OH}^2) \quad (21)$$

$$S_{H_2O} = 2W_{H_2O} (k_{f2}C_{OH}^2C_{H_2} - k_{b2}C_{H_2O}^2) \quad (22)$$

$$S_{H_2} = W_{H_2} \left(\frac{S_{O_2}}{W_{O_2}} - \frac{1}{2} \frac{S_{H_2O}}{W_{H_2O}} \right) \quad (23)$$

$$S_{OH} = -W_{OH} \left(2 \frac{S_{O_2}}{W_{O_2}} + \frac{S_{H_2O}}{W_{H_2O}} \right) \quad (24)$$

where $C_i = \frac{\rho Y_i}{W_i}$ denotes the concentration of species i .

By observing Eq. (21) - (24), one can notice that the rate of formation (production) of any given species depends only on the concentrations of the other modeled species, and that the rate of consumption (destruction) of that species always depends on its own concentration (among others). As a result, the diagonal entries of the chemical source-term Jacobian are always negative (at least for the mechanisms modeled in this work).

Theorem 3.1 *Let $\tilde{D} \approx \left(\frac{\partial S_{i=1 \dots N_s-1}}{\partial (\rho Y)} \right)$ denote an approximation to the full source-term Jacobian, consisting of either the lower or upper triangular, or diagonal portions of the full Jacobian, $\frac{\partial S_{i=1 \dots N_s-1}}{\partial (\rho Y)}$, then the eigenvalues of \tilde{D} are necessarily negative.*

Proof Since \tilde{D} is triangular, its eigenvalues, λ_i , are the entries on the main diagonal, $\tilde{D}_{i,i}$ [63]. Combined with the above observations regarding the diagonal entries of the chemical source-term Jacobian, the proof is complete.

Based on this reasoning, it is advantageous to employ a diagonal or lower-triangular approximation to the full source term Jacobian for implicit time-integration. Indeed, Kim²⁵ and Kim et al.²⁶ have reported better convergence and stability characteristics when using lower-triangular approximations, compared to that obtained with the full Jacobian. However, the performance obtained with a triangular approximation is highly dependent on the species ordering, and is thus difficult to extend to arbitrary large reaction mechanisms. Moreover, a triangular approximation would hamper the desired block diagonal structure of the implicit operator. Therefore, a diagonal approximation of the full chemical source-term Jacobian is proposed in this work, as follows:

$$\tilde{D} = \text{Diag} \left(\frac{\partial S_{i=1 \dots N_s-1}}{\partial (\rho Y)} \right) \quad (25)$$

4 Numerical Simulation Results

In this section, the performance of the proposed numerical framework is evaluated through simulation of several well-known test cases of supersonic combustion. The aim of the tests is to study the convergence characteristics of the proposed diagonal approximation of the chemical reactions Jacobian, with respect to the full, analytic Jacobian.

4.1 Supersonic Combustion in a Ramped Duct

The first test case simulated in this work involves the supersonic combustion of a premixed, stoichiometric hydrogen/air mixture flowing over a 10° viscous ramp. This is a common theoretical test case for supersonic combustion, with several published sets of numerical results [18, 64, 65]. The free-stream (inlet) conditions are: $M_\infty = 4$, $T_\infty = 900K$, $P_\infty = 1 \text{ atm}$, and $Re = 2 \cdot 10^7$. The dimensions of the ramp, along with the (coarse) computational domain are shown in Figure 1. Common grid parameters are given in Table 1. To avoid an abrupt change in velocity at the boundary layers near the inlet boundary, an inviscid duct with a length of 0.4 cm was added before the actual viscous duct.

Name	Dim.	Δy_1	y^+
Coarse grid	109×101	$4 \times 10^{-5} \text{ cm}$	≤ 0.3
Fine grid	109×161	$7 \times 10^{-5} \text{ cm}$	≤ 0.45

Table 1: Ramped-duct computational grid parameters

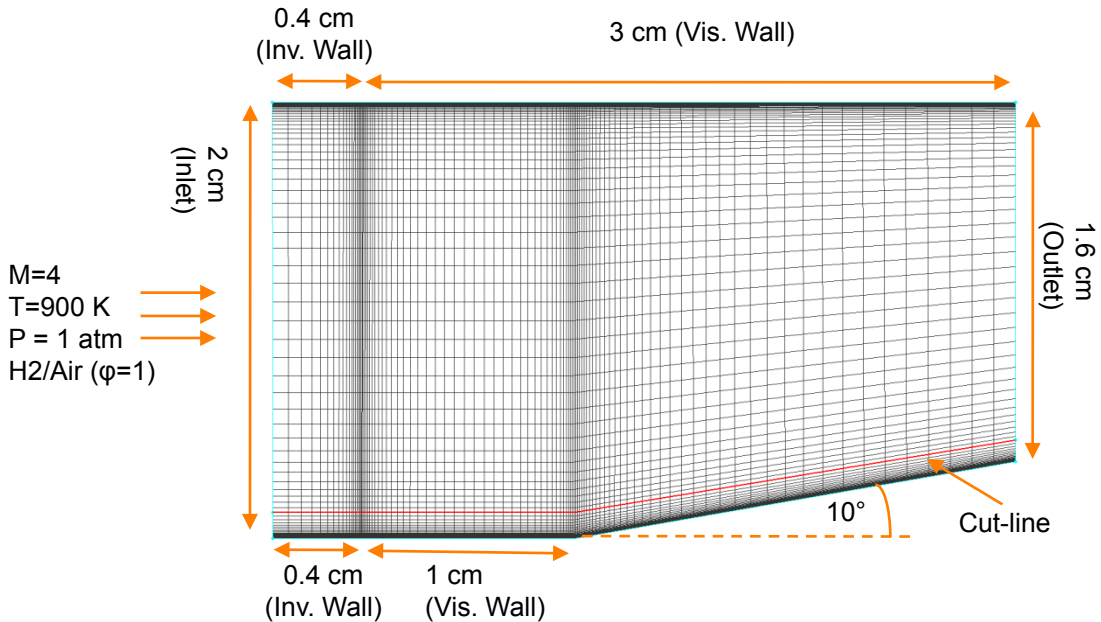


Figure 1: Coarse computational grid and set-up used in the simulations of supersonic combustion in a 10° -ramped duct. — marks the cut-line located 0.13 cm from the lower wall, along which temperature and mass fractions distributions are reported.

This flow was computed using Stahl and Warnatz's [46] detailed nine-species, 18-reactions model, assuming laminar chemistry (i.e., neglecting turbulence-chemistry interaction). The assumption of laminar chemistry is valid as the turbulent Damköhler number is extremely small in this case ($Da_T \approx 10^{-5} \ll 1$).

Nevertheless, the $k - \omega$ turbulence model was used to model the effects of turbulence on the mean-flow. In addition, the effects of viscosity, heat conduction, and species diffusion were also included, resulting in a computationally intensive simulation.

The myriad of physical phenomena that have to be accurately modeled render this case extremely challenging. The turbulent boundary layers must be correctly resolved, thus requiring significant clustering of cells near the duct walls, leading to anisotropy due to highly stretched (aspect ratio ≈ 1500) cells. Proper resolution of shockwave-boundary layer interactions (SBLI) and accurate capturing of the oblique shock are also essential to correctly determine the combustion front. Finally, the correct modeling of species diffusion is imperative for obtaining accurate combustion propagation. The results presented herein were all obtained with the coarser grid, as it was closer in dimensions to the one that was used by Ju⁶⁵. Since experimental data is not available for this case, the results of Ju⁶⁵ were used as reference for verification purposes.

Numerically obtained iso-pressure contours are shown in Figure 2, and the distributions of temperature and mass fractions along the cut-line (marked in Figure 1) are given in Figure 3.

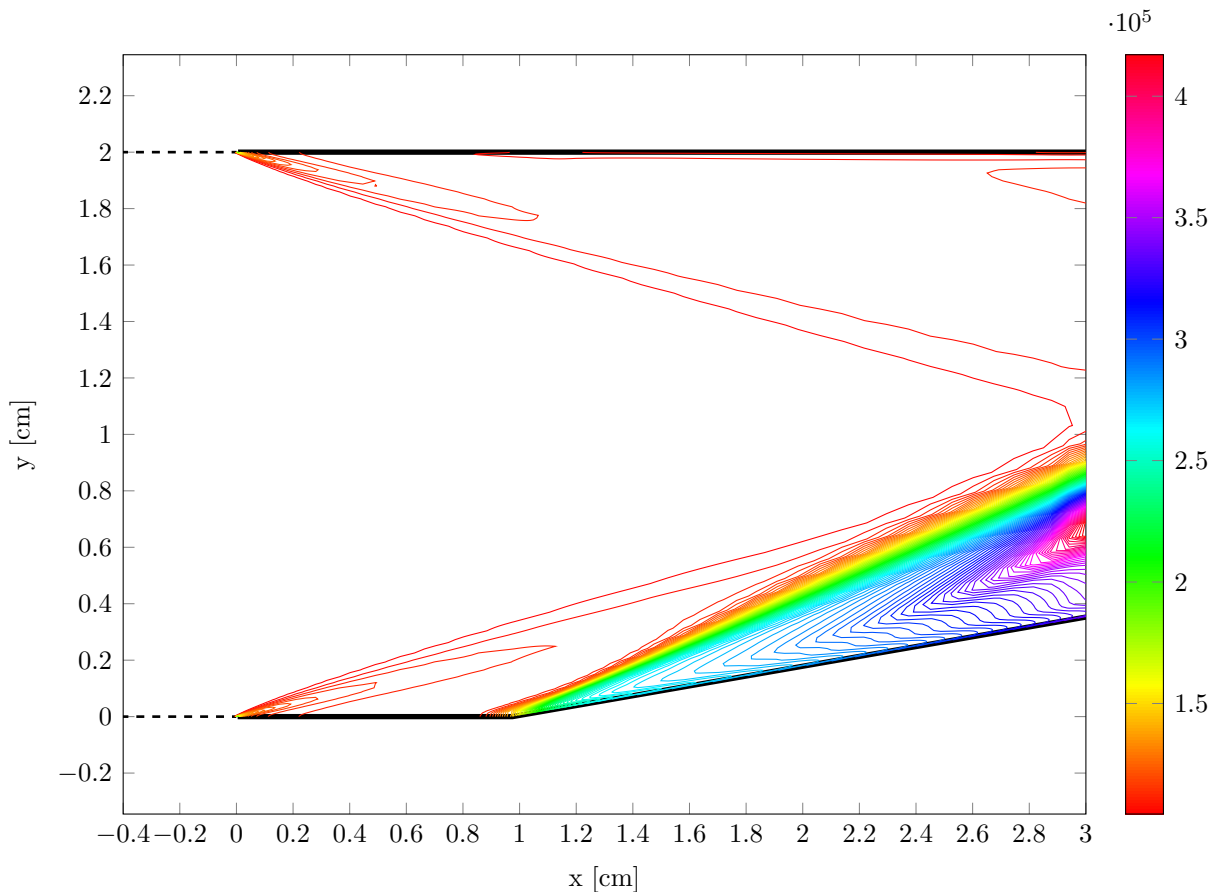


Figure 2: Iso-pressure (Pa) contours of supersonic combustion in a ramped duct (coarse grid).

At first, the free stream temperature is not high enough to initiate a reaction, but the combination of higher temperature in the boundary layer, along with a rise in temperature due to crossing of the oblique shock, trigger a reaction between hydrogen and oxygen in the vicinity of the lower ramp wall. Both constituents are almost fully consumed in this case. The distributions of temperature and mass fractions along the cut-line are in good agreement with published results by Ju⁶⁵. A slight discrepancy in the predicted level of hydroxyl (OH) radical formation is evident, probably related to the different hydrogen combustion model (9 species, 33 reactions) that was used in Ref. [65].

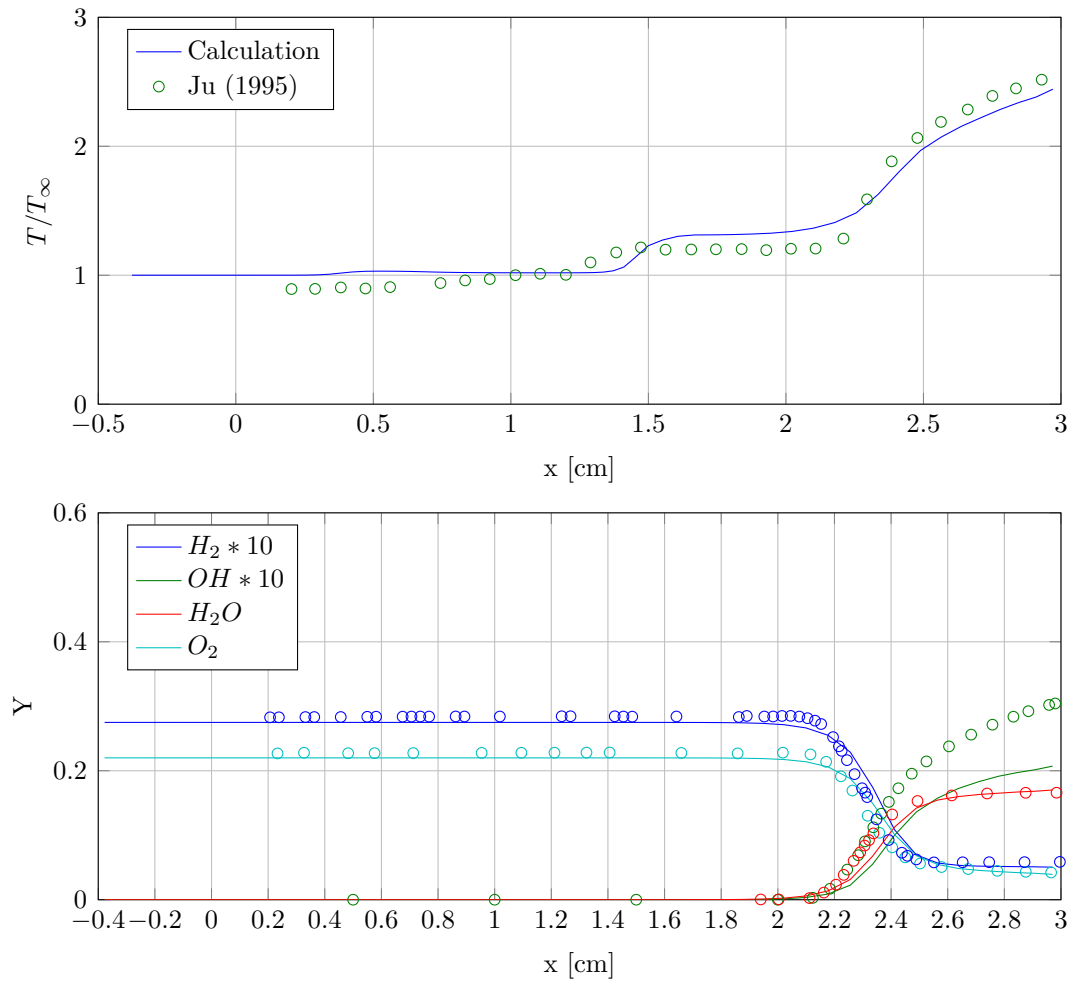


Figure 3: Calculated temperature and mass fraction distributions for the supersonic combustion of H_2/Air in a ramped duct. —, current computation; \circ , numerical results from [65].

Aside from the strong oblique shock due to the ramp, a weak oblique shock is also formed at the left edge of the domain ($x=0$) due to the displacement thickness of the boundary layer. Beyond the oblique shock, downstream of the ramp corner, the increased temperature and pressure lead to rapid reactions, heat release and production of radicals. The increased diffusion of those radicals and heat to the cold areas further away from the ramp wall result in a combustion front that gradually moves away from the wall. The curved combustion front may be observed in the plots of iso-temperature (Figure 4(a)) and iso-water-vapor fraction (Figure 4(b)). Also worth noting is the fact that rapid combustion takes place in the boundary layer, even before the flow reaches the ramp, as indicated by the water-vapor mass fractions. This is a result of the high kinetic energy of the free-stream flow, which transforms to thermal energy in the boundary layer, ultimately triggering chemical reactions.

A comparison of convergence histories obtained for this case with the proposed diagonal approximation and the full, analytic chemical source-term Jacobians is presented in Figure 5. For this case, the diagonal approach proved to be superior in terms of asymptotic convergence rate and maximum allowed CFL number. When taking into account the additional computational cost involved in computing the inverse of the dense, analytic chemical source-term Jacobian at each cell, and in every iteration, the benefit in employing the diagonal approach is even more accentuated.

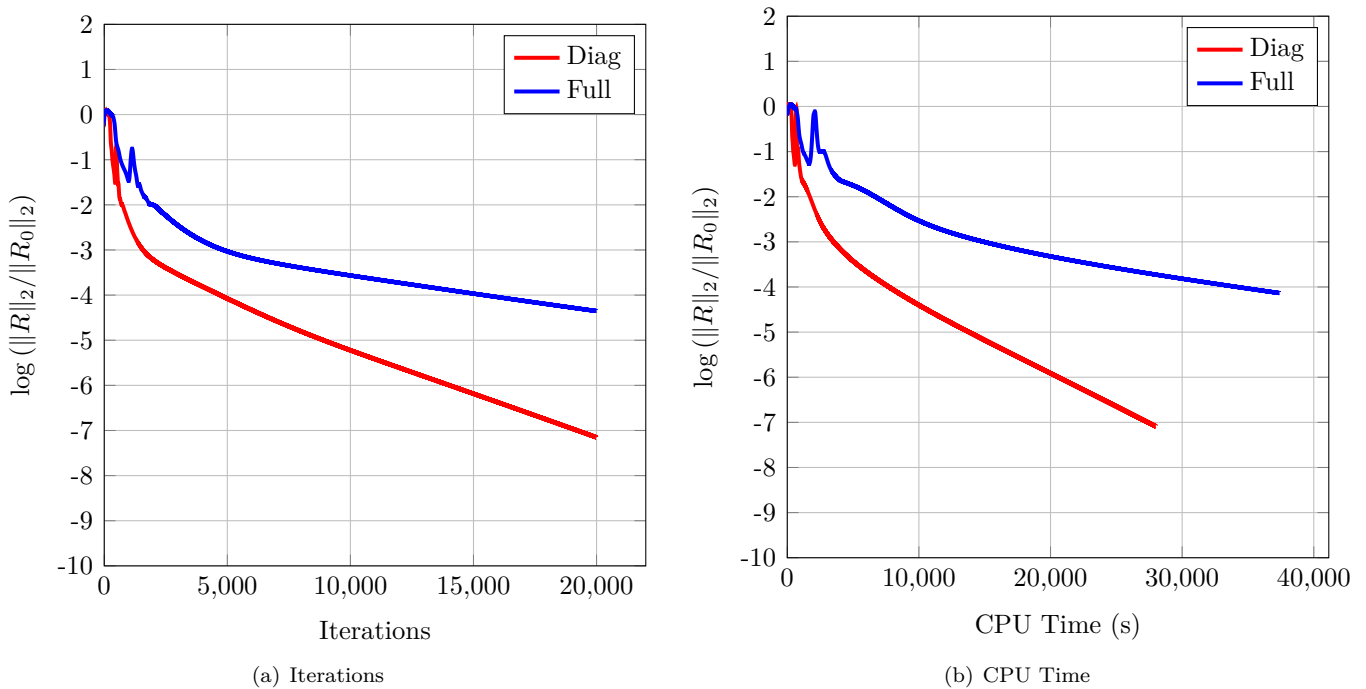
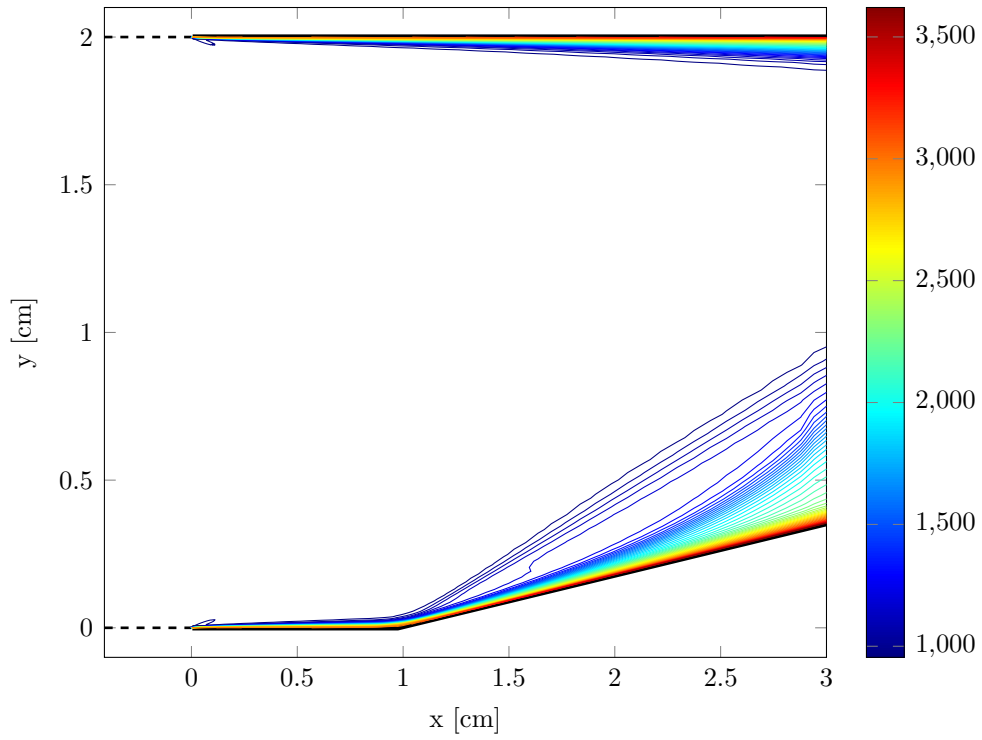
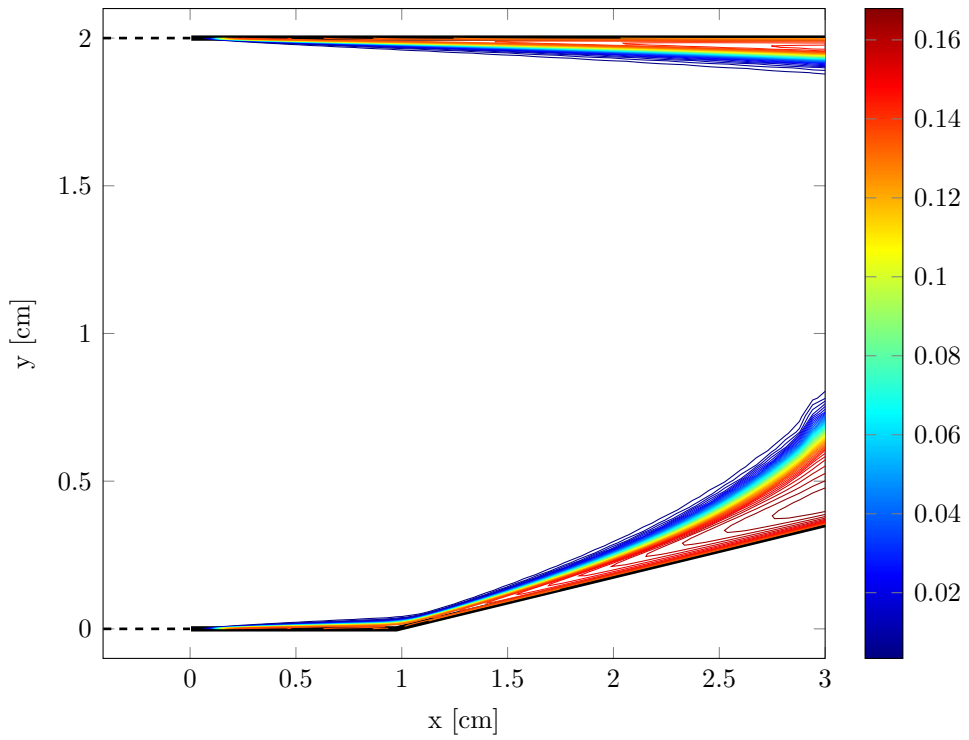


Figure 5: Comparison of convergence histories obtained with the proposed diagonal and full chemical source-term Jacobians for the case of $M = 4$, H_2/Air supersonic combustion in a ramped duct



(a) Temperature (K)



(b) H_2O Fractions

Figure 4: Iso-water-vapor fraction and Iso-temperature contours obtained in simulation of $M = 4$, H_2/Air supersonic combustion in a ramped duct.

4.2 Supersonic Diffusion Flame

The second test case is a reproduction of the experiment conducted by Cheng et al. [66], in which measurements of mixing and finite-rate reaction rates were conducted for a non-premixed, supersonic hydrogen-air diffusion flame. This is a well-known test case of supersonic combustion that has been extensively studied both experimentally [66] and numerically [67–69].

The experimental setup of Cheng et al. [66] is sketched in Figure 6. Two co-axial jets of vitiated air (outer) and hydrogen (inner) are mixed in the burner. The vitiated air stream is accelerated through a converging-diverging nozzle and reaches Mach 2 at a temperature of 1250 K at the entrance to the burner. Experimental measurements of major species mass fractions (N_2 , O_2 , H_2 , H_2O , OH) and of temperature are available at 7 downstream planes.

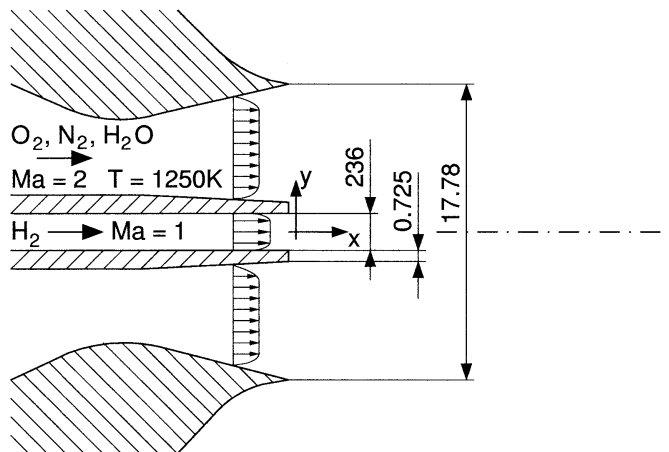


Figure 6: Schematic description of the Cheng et al. [66] supersonic diffusion flame experiment

An axisymmetric flow simulation is conducted, in accordance with the nature of the flow. The converging-diverging section is not modeled and uniform properties (i.e., velocity and temperature) are assumed throughout the entrance plane of the hydrogen stream (inner jet). The inner and outer burner lip surface are assumed adiabatic and non-catalytic. A steady-state simulation is conducted based on experimental observations regarding the existence of a quasi-steady flame structure.

This flow was computed using Jachimowski’s reduced model [47], assuming laminar chemistry (i.e., neglecting turbulence-chemistry interaction). The $k - \omega$ turbulence model was again used to model the effects of turbulence on the mean-flow.

The shear layer formed between the hydrogen and vitiated air jets is responsible for the mixing and subsequent combustion of the flow. The structure of the resulting lifted flame may be seen in Figure 8.

Figure 10 compares the mean temperature and OH mole fraction profiles with the experimental measurements at an axial station of $X/D = 43.1$. The comparisons with experiment are generally favorable, considering that accurate simulation of this test case usually requires the use of assumed PDF models [69, 70] which were beyond the scope of the current work.

A comparison of convergence histories obtained for this case with the proposed diagonal approximation and the full, analytic chemical source-term Jacobians is presented in Figure 11. For this case, both approaches (i.e., diagonal approximation and full Jacobian) yield similar convergence rates in terms of iterations. However, when taking into account the additional computational cost involved in computing the inverse of the dense, analytic chemical source-term Jacobian at each cell, and in every iteration, a clear benefit is demonstrated towards the diagonal approach.

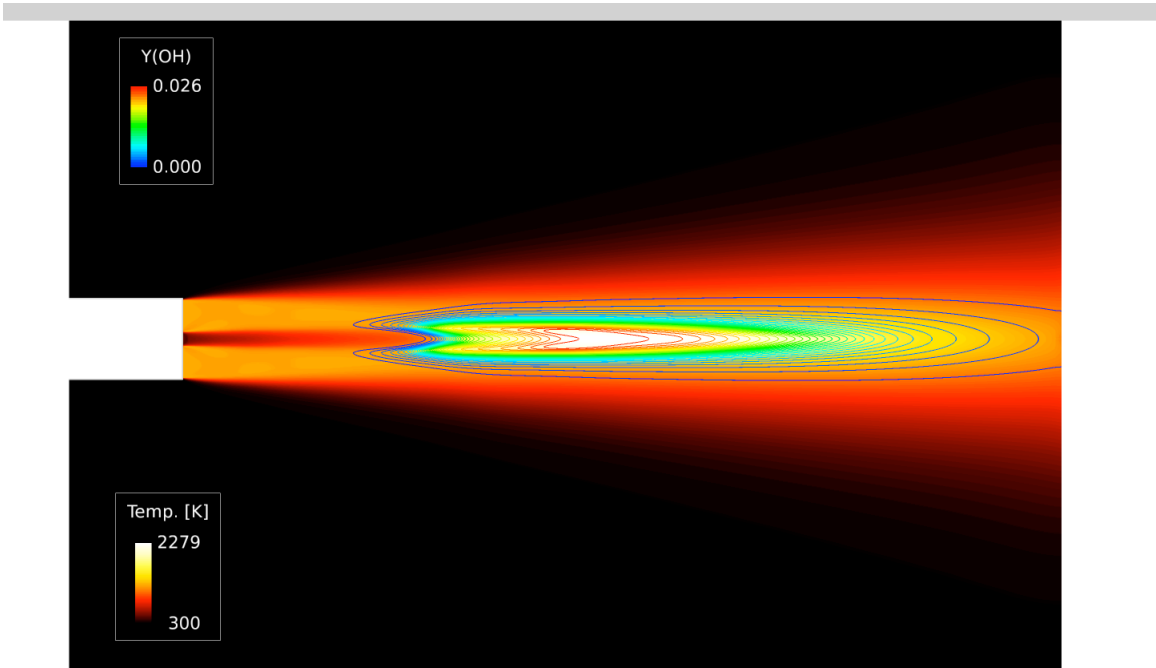


Figure 7: Numerically obtained temperature distribution overlaid by Iso-*OH*-mass-fraction contours in simulation of the supersonic diffusion flame

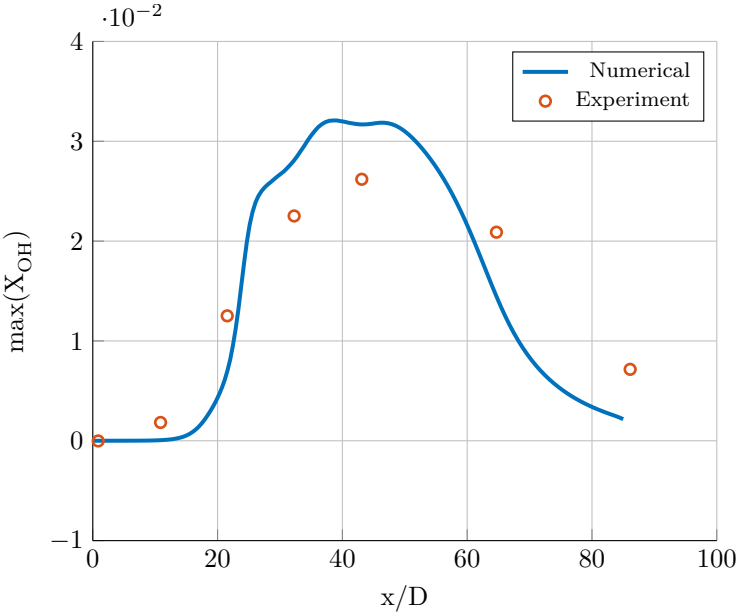
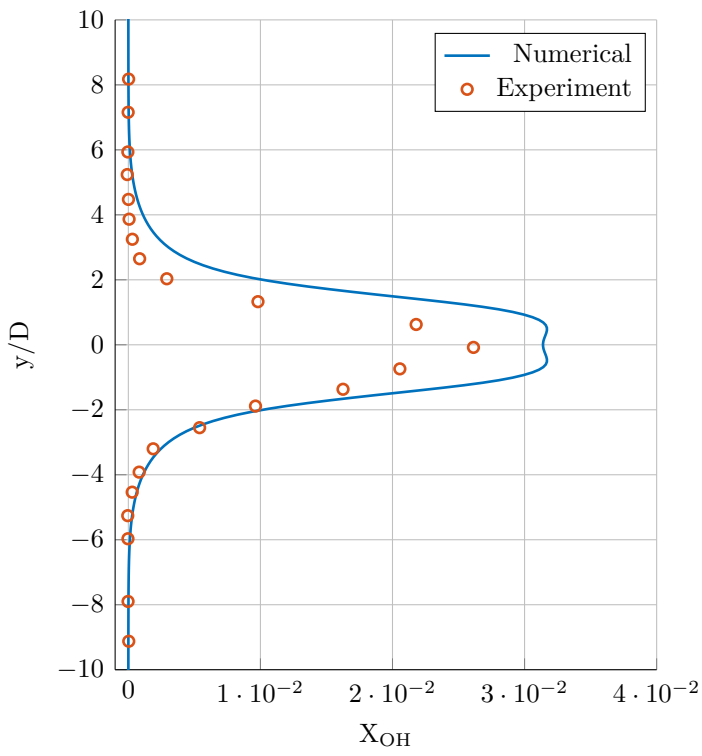
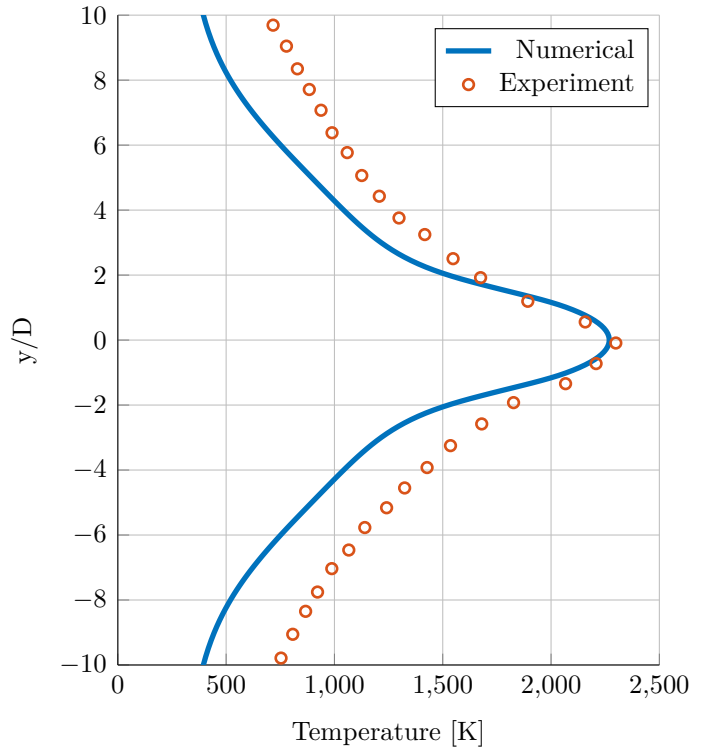


Figure 8: Comparison of numerically obtained (-) maximum *OH* mole fractions with experimental measurements (o) of Cheng et al. [66]



(a) OH Mole Fraction



(b) Temperature

Figure 9: Comparison of numerically obtained (-) and experimentally measured (\circ , [66]) flame properties at $X/D = 43.1$ axial position of the supersonic diffusion flame.

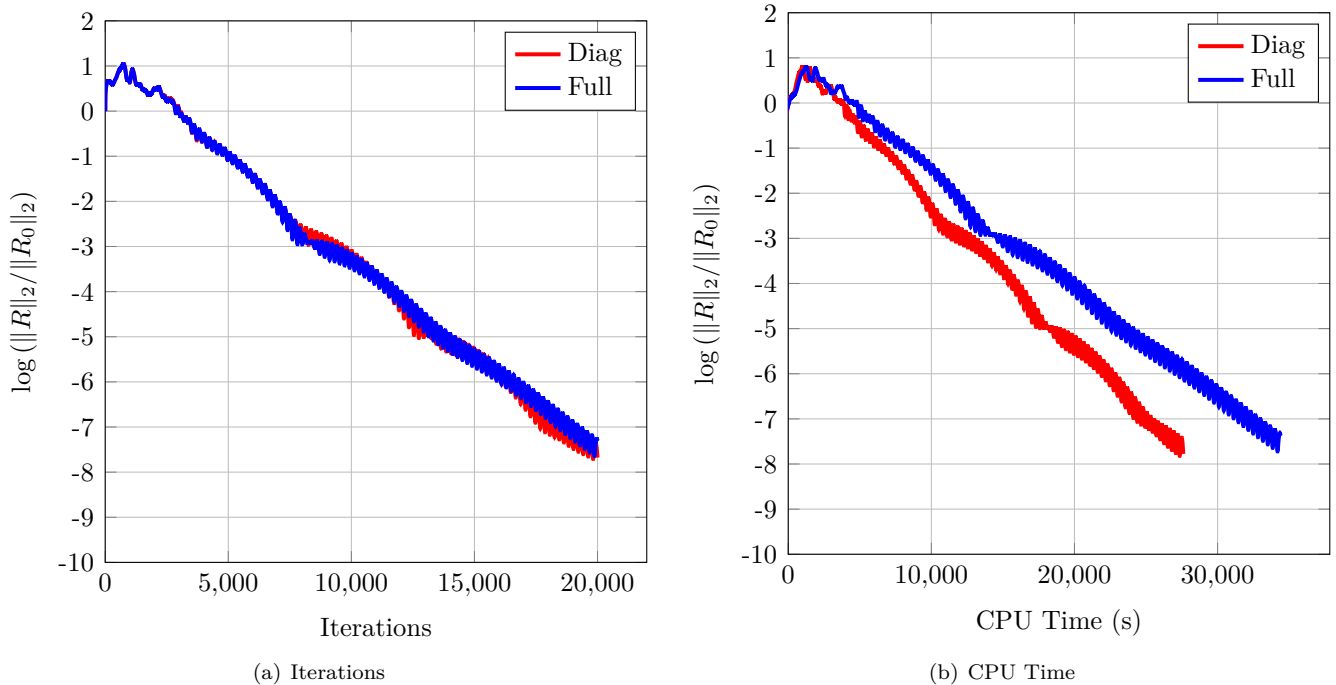


Figure 10: Comparison of convergence histories obtained with the proposed diagonal and full chemical source-term Jacobians for the supersonic diffusion flame test case

5 Summary

A novel, robust numerical framework for the simulation of supersonic combustion is developed. The iterative solution is highly efficient thanks to the decoupled implicit solution of the mean-flow (Navier-Stokes) and chemistry model equations, especially when large reaction mechanisms are employed. The diagonal approximation of the full implicit operator significantly reduces the computational cost, without significantly affecting stability and convergence rates in steady-state, chemically reacting flow simulations.

Results obtained from the simulation of two-dimensional and axisymmetric, supersonic combustion cases are presented. The obtained numerical results favorably agree with experimental measurements in the simulation of a non-premixed supersonic diffusion flame. Finally, The extended UPC implicit scheme, together with the proposed diagonal approximation of the chemical source-term Jacobian, enables the use of higher CFL numbers in the premixed combustion test case, and offers a considerable reduction in the computational time required to obtain iterative convergence, with respect to an equivalent scheme that is based on a full, analytic formulation of the chemical source-term Jacobian.

References

- [1] G. Tchuente and D. E. Zeitoun. “Effects of Chemistry in Nonequilibrium Hypersonic Flow Around Blunt Bodies”. In: *Journal of Thermophysics and Heat Transfer* **23**:3 (2009), 433–442 (cited on p. 2)
- [2] F. Bisetti. “Integration of large chemical kinetic mechanisms via exponential methods with Krylov approximations to Jacobian matrix functions”. In: *Combustion Theory and Modelling* **16**:3 (2012), 387–418 (cited on p. 2)
- [3] V. R. Katta and W. M. Roquemore. “Calculation of multidimensional flames using large chemical kinetics”. In: *AIAA journal* **46**:7 (2008), 1640–1650 (cited on pp. 2, 4)

- [4] C. W. Gear. *Numerical Initial Value Problems in Ordinary Differential Equations*. Prentice Hall PTR, 1971 (cited on p. 2)
- [5] H. Lomax, T. H. Pulliam, and D. W. Zingg. *Fundamentals of computational fluid dynamics*. Springer Berlin, 2001 (cited on p. 2)
- [6] T. R. Bussing. “A Finite Volume Method for the Navier-Stokes Equations with Finite Rate Chemistry”. PhD thesis. Massachusetts Institute of Technology, 1985 (cited on p. 3)
- [7] Z.-N. Wu and S. Fu. “Positivity of k -epsilon turbulence models for incompressible flow”. In: *Mathematical Models and Methods in Applied Sciences* **12**:3 (2002), 393–406 (cited on p. 3)
- [8] L. C. Scalabrin. “Numerical Simulation of Weakly Ionized Hypersonic Flow Over Reentry Capsules”. PhD thesis. University of Michigan, 2007 (cited on pp. 3, 9)
- [9] X. Gao. “A Parallel Solution-adaptive Method for Turbulent Non-premixed Combusting Flows”. PhD thesis. University of Toronto, 2008 (cited on p. 3)
- [10] Y. Mor-Yossef and Y. Levy. “Unconditionally positive implicit procedure for two-equation turbulence models: Application to k - ω turbulence models”. In: *Journal of Computational Physics* **220**:1 (2006), 88–108 (cited on pp. 3, 5, 10)
- [11] Y. Mor-Yossef and Y. Levy. “The unconditionally positive-convergent implicit time integration scheme for two-equation turbulence models: Revisited”. In: *Computers & Fluids* **38**:10 (2009), 1984–1994 (cited on pp. 3, 10)
- [12] A. Berman and R. J. Plemmons. *Nonnegative matrices in the mathematical sciences*. Computer Science and Applied Mathematics. Academic Press, Inc., 1979 (cited on p. 3)
- [13] T. R. Bussing and E. M. Murman. “Finite-volume method for the calculation of compressible chemically reacting flows”. In: *AIAA journal* **26**:9 (1988), 1070–1078 (cited on p. 3)
- [14] S.-s. Kim, C. Kim, and O.-H. Rho. “Multigrid Algorithm for Computing Hypersonic, Chemically Reacting Flows”. In: *Journal of Spacecraft and Rockets* **38**: (2001), 865–874 (cited on p. 4)
- [15] X. Gao and C. P. T. Groth. “A parallel adaptive mesh refinement algorithm for predicting turbulent non-premixed combusting flows”. In: *International Journal of Computational Fluid Dynamics* **20**:5 (2006), 349–357 (cited on p. 4)
- [16] M. Deepu, S. Gokhale, and S. Jayaraj. “Numerical Modeling of Scramjet Combustor Flow Field Using Unstructured Point Implicit Finite Volume Method”. In: *44th AIAA Aerospace Sciences Meeting and Exhibit*. American Institute of Aeronautics and Astronautics, 2012 (cited on p. 4)
- [17] S. Yoon and A. Jameson. “An LU-SSOR scheme for the Euler and Navier-Stokes equations”. In: *25th AIAA Aerospace Sciences Meeting*. 1987 (cited on p. 4)
- [18] J. S. Shuen and S. Yoon. “Numerical study of chemically reacting flows using a lower-upper symmetric successive overrelaxation scheme”. In: *AIAA journal* **27**:12 (1989), 1752–1760 (cited on pp. 4, 12)
- [19] S. Yoon and A. Jameson. “Lower-Upper Symmetric Gauss-Seidel Method for the Euler and Navier-Stokes Equations”. In: *AIAA journal* **26**:9 (1988) (cited on p. 4)
- [20] M. J. Wright, G. V. Candler, and D. Bose. “Data-parallel line relaxation method for the Navier-Stokes equations”. In: *AIAA journal* **36**:9 (1998), 1603–1609 (cited on pp. 4, 5)
- [21] M. MacLean and T. White. “Implementation of Generalized Minimum Residual Krylov Subspace Method for Chemically Reacting Flows”. In: *50th AIAA Aerospace Sciences Meeting including the New Horizons Forum and Aerospace Exposition*. 2012 (cited on p. 4)
- [22] C. Park and S. Yoon. “Fully coupled implicit method for thermochemical nonequilibrium air at sub-orbital flight speeds”. In: *Journal of Spacecraft and Rockets* **28**:1 (1991), 31–39 (cited on p. 4)
- [23] S. Eberhardt and S. Imlay. “Diagonal implicit scheme for computing flows with finite rate chemistry”. In: *Journal of Thermophysics and Heat Transfer* **6**:2 (1992), 208–216 (cited on p. 4)

- [24] J. R. Edwards. “An Implicit Multigrid Algorithm for Computing Hypersonic, Chemically Reacting Viscous Flows”. In: *Journal of Computational Physics* **123**:1 (1996), 84–95 (cited on p. 4)
- [25] C. Kim. “Approximate Jacobian Methods for Efficient Calculation of Reactive Flows”. In: *36th AIAA/ASME/SAE/ASEE Joint Propulsion Conference & Exhibit*. 2001, 1–10 (cited on pp. 4, 10, 11)
- [26] S.-L. Kim, I.-S. Jeung, and Y.-H. Choi. “Partially implicit scheme for chemically reacting flows at all Mach numbers”. In: *AIAA journal* **39**:10 (2001), 1893–1900 (cited on pp. 4, 10, 11)
- [27] C. Lian, G. Xia, and C. L. Merkle. “Impact of source terms on reliability of CFD algorithms”. In: *Computers & Fluids* **39**:10 (2010), 1909–1922 (cited on pp. 4, 11)
- [28] N. N. Yanenko. *The Method of Fractional Steps*. Springer-Verlag, 1971 (cited on p. 4)
- [29] G. Strang. “On the Construction and Comparison of Difference Schemes”. In: *SIAM Journal on Numerical Analysis* **5**:3 (1968), 506–517 (cited on p. 4)
- [30] M. A. Singer, S. B. Pope, and H. N. Najm. “Operator-splitting with ISAT to model reacting flow with detailed chemistry”. In: *Combustion Theory and Modelling* **10**: (2006), 199–217 (cited on p. 4)
- [31] S. B. Pope and Z. Ren. “Efficient Implementation of Chemistry in Computational Combustion”. In: *Flow, Turbulence and Combustion* **82**: (2009), 437–453 (cited on p. 4)
- [32] D. A. Schwer, P. Lu, and W. H. Green. “A consistent-splitting approach to computing stiff steady-state reacting flows with adaptive chemistry”. In: *Combustion Theory and Modelling* **7**:2 (2003), 383–399 (cited on p. 4)
- [33] S. G. Sheffer, A. Jameson, and L. Martinelli. “An Efficient Multigrid Algorithm for Compressible Reactive Flows”. In: *Journal of Computational Physics* **144**: (1998), 484–516 (cited on p. 5)
- [34] P. A. Gnoffo. *An upwind-biased, point-implicit relaxation algorithm for viscous, compressible perfect-gas flows*. Tech. rep. 1990 (cited on p. 5)
- [35] B. Kirk, R. Stogner, T. A. Oliver, and P. T. Bauman. “Recent Advancements in Fully Implicit Numerical Methods for Hypersonic Reacting Flows”. In: *21st AIAA Computational Fluid Dynamics Conference*. American Institute of Aeronautics and Astronautics, 2013 (cited on p. 5)
- [36] G. V. Candler, P. K. Subbareddy, and I. Nompelis. “Decoupled Implicit Method for Aerothermodynamics and Reacting Flows”. In: *AIAA journal* **51**:5 (2013), 1245–1254 (cited on pp. 5, 9)
- [37] M. Wasserman, Y. Mor-Yossef, and J. B. Greenberg. “A positivity-preserving, implicit defect-correction multigrid method for turbulent combustion”. In: *Journal of Computational Physics* **316**:C (2016), 303–337 (cited on pp. 5, 10)
- [38] K. A. Hoffmann, S. T. Chiang, S. Siddiqui, and M. Papadakis. *Fundamental equations of fluid mechanics*. Engineering Education System, 1996 (cited on p. 5)
- [39] J. O. Hirschfelder and C. F. Curtiss. *Molecular theory of gases and liquids*. Wiley, 1964 (cited on p. 6)
- [40] B. Reimann and V. Hannemann. “Numerical investigation of double-cone and cylinder experiments in high enthalpy flows using the DLR TAU code”. In: *48th AIAA Aerospace Sciences Meeting Including the New Horizons Forum and Aerospace Exposition*. AIAA Paper 2010-1282, 2010 (cited on p. 6)
- [41] C. R. Wilke. “A viscosity equation for gas mixtures”. In: *Journal of Chemical Phys* **18**: (1950), 517 (cited on p. 6)
- [42] M. J. Wright, D. Bose, G. E. Palmer, and E. Levin. “Recommended collision integrals for transport property computations - part 1: air species”. In: *AIAA journal* **43**:12 (2005), 2558–2564 (cited on p. 6)
- [43] M. Capitelli, C. Gorse, S. Longo, and D. Giordano. “Collision integrals of high-temperature air species”. In: *Journal of Thermophysics and Heat Transfer* **14**:2 (2000), 259–268 (cited on p. 6)
- [44] R. J. Kee, M. E. Coltrin, and P. Glarborg. *Chemically Reacting Flow: Theory and Practice*. John Wiley & Sons, 2005 (cited on p. 6)

- [45] A. Burcat and B. Ruscic. *Third Millenium Ideal Gas and Condensed Phase Thermochemical Database for Combustion with Updates from Active Thermochemical Tables*. Tech. rep. TAE 960. 2005 (cited on p. 6)
- [46] G. Stahl and J. Warnatz. “Numerical investigation of time-dependent properties and extinction of strained methane- and propane-air flamelets”. In: *Combustion and flame* **85**:3-4 (1991), 285–299 (cited on pp. 7, 12)
- [47] C. J. Jachimowski. “An analytical study of the hydrogen-air reaction mechanism with application to scramjet combustion”. In: (1988) (cited on pp. 7, 17)
- [48] J. C. Kok. “Resolving the dependence on freestream values for the $k\text{-}\omega$ turbulence model”. In: *AIAA journal* **38**:7 (2000), 1292–1295 (cited on p. 7)
- [49] Y. Wada and M.-S. Liou. “A Flux Splitting Scheme with High-resolution and Robustness for Discontinuities”. In: *32th AIAA Aerospace Science Meeting and Exhibit*. Reno, NV, 1994, 23 (cited on p. 8)
- [50] B. van Leer. “Towards the ultimate conservative difference scheme. V. A second-order sequel to Godunov’s method”. In: *Journal of Computational Physics* **32**:1 (1979), 101–136 (cited on p. 8)
- [51] B. van Leer. “Upwind-difference methods for aerodynamic problems governed by the Euler equations”. In: *Large-Scale Computations in Fluid Mechanics; Proceedings of the Fifteenth Summer Seminar on Applied Mathematics*. 1985, 327–336 (cited on p. 8)
- [52] G. D. van Albada, B. van Leer, and W. W. Roberts. “A comparative study of computational methods in cosmic gas dynamics”. In: *Astronomy and Astrophysics* **108**:1 (1982), 76–84 (cited on p. 8)
- [53] P. Jawahar and H. Kamath. “A High-Resolution Procedure for Euler and NavierStokes Computations on Unstructured Grids”. In: *Journal of Computational Physics* **164**:1 (2000), 165–203 (cited on p. 8)
- [54] Y. Mor-Yossef. “Turbulent Flow Simulations on Unstructured Grids using a Reynolds Stress Model”. In: *22nd AIAA Computational Fluid Dynamics Conference*. AIAA Paper 2015-2761: American Institute of Aeronautics and Astronautics, 2015 (cited on p. 8)
- [55] P. Batten, M. A. Leschziner, and U. C. Goldberg. “Average-state Jacobians and implicit methods for compressible viscous and turbulent flows”. In: *Journal of Computational Physics* **137**:1 (1997), 38–78 (cited on pp. 8, 9)
- [56] J. Wackers and B. Koren. “Multigrid Solution Method for the Steady RANS Equations”. In: *Journal of Computational Physics* **226**: (2007), 25 (cited on p. 9)
- [57] S. Lee and D. W. Choi. “On coupling the Reynolds-averaged Navier-Stokes equations with two-equation turbulence model equations”. In: *International Journal for Numerical Method in Fluids* **50**:2 (2006), 165–197 (cited on p. 9)
- [58] H. C. Yee, G. H. Klopfer, and J. L. Montagné. “High-resolution shock-capturing schemes for inviscid and viscous hypersonic flows”. In: *Journal of Computational Physics* **88**:1 (1990), 31–61 (cited on p. 9)
- [59] J. L. Steger and R. F. Warming. “Flux vector splitting of the inviscid gasdynamic equations with application to finite-difference methods”. In: *Journal of Computational Physics* **40**:2 (1981), 263–293 (cited on p. 9)
- [60] J. R. Amaladas and H. Kamath. “Implicit and multigrid procedures for steady-state computations with upwind algorithms”. In: *Computers & Fluids* **28**:2 (1999), 187–212 (cited on p. 9)
- [61] C. L. Merkle, M. Deshpande, and S. Venkateswaran. “Efficient implementation of turbulence modeling in computational schemes”. In: *Proceedings of the Second U.S. National Congress on Computational Mechanics*. Pergamon, Oxford, 1993 (cited on p. 11)
- [62] R. C. Rogers and W. Chinitz. “Using a global hydrogen-air combustion model in turbulent reacting flow calculations”. In: *20th Aerospace Sciences Meeting* **21**:4 (1983), 586–591 (cited on p. 11)
- [63] S. Axler. *Linear Algebra Done Right*. Springer, 1997 (cited on p. 11)

- [64] T. Chitsomboon, A. Kumar, and S. N. Tiwari. “Numerical Study of Finite-Rate Supersonic Combustion Using Parabolized Equations”. In: *25th AIAA Aerodynamic Measurement Technology and Ground Testing Conference*. Reno, NV, 1987 (cited on p. 12)
- [65] Y. Ju. “Lower-upper scheme for chemically reacting flow with finite rate chemistry”. In: *AIAA journal* **33**:8 (1995), 1418–1425 (cited on pp. 12–14)
- [66] T. S. Cheng, J. A. Wehrmeyer, R. W. Pitz, and O. Jarrett. “Raman measurement of mixing and finite-rate chemistry in a supersonic hydrogen-air diffusion flame”. In: *Combustion and flame* **99**: (1994), 157–173 (cited on pp. 17–19)
- [67] R. A. Baurle, A. T. Hsu, and H. A. Hassan. “Assumed and evolution probability density functions in supersonic turbulent combustion calculations”. In: *Journal of Propulsion and Power* **11**:6 (1995), 1132–1138 (cited on p. 17)
- [68] C. J. Roy. *A computational study of turbulent reacting flowfields for scramjet applications*. 1998 (cited on p. 17)
- [69] H. Mobus, P. Gerlinger, and D. Bruggemann. “Scalar and joint scalar-velocity-frequency Monte Carlo PDF simulation of supersonic combustion”. In: *Combustion and flame* **132**:1 (2003), 3–24 (cited on p. 17)
- [70] R. A. Baurle. *Modeling of turbulent reacting flows with probability density functions for scramjet applications*. 1995 (cited on p. 17)